Riparian and in-stream controls on nutrient concentrations and fluxes in a headwater forested stream.

Authors: S. Bernal[1*], A. Lupon[2], M. Ribot[1], F. Sabater[2], E. Martí[1]

Affiliations:

[1]Center for Advanced Studies of Blanes (CEAB-CSIC), Accés a la Cala Sant Francesc 14, 17300, Blanes, Girona, Spain.

[2]Departament d'Ecologia, Facultat de Biologia, Universitat de Barcelona, Av. Diagonal 643, 08028, Barcelona, Spain.

*corresponding author: sbernal@ceab.csic.es

Keywords: headwater stream, dissolved inorganic nitrogen, phosphorus, longitudinal variation, riparian groundwater, in-stream net nutrient cycling.

Abstract

Headwater streams are recipients of water sources draining through terrestrial ecosystems. At the same time, stream biota can transform and retain nutrients dissolved in stream water. Yet, studies considering simultaneously these two sources of variation of stream nutrient chemistry are rare. To fill this gap of knowledge, we analyzed stream water and riparian groundwater concentrations and fluxes as well as in-stream net uptake rates for nitrate (NO_3^-), ammonium (NH_4^+), and soluble reactive phosphorus (SRP) along a 3.7-km reach on an annual basis. Chloride concentrations (used as conservative tracer) indicated a strong hydrological connection at the riparian-stream interface. However, stream and riparian groundwater nutrient concentrations showed a moderate to null correlation, suggesting high in-stream biogeochemical processing. In-stream net nutrient uptake (F_{sw}) modified median stream input fluxes by 6, 18, and 20% for NO_3^-, NH_4^+, and SRP, respectively. For the three nutrients, F_{sw} was highly variable across contiguous segments and over time, but its temporal variation was not related to the vegetative period of the riparian forest. For NH_4^+, the occurrence of $F_{sw} > 0$ μg N m^{-1} s^{-1} (gross uptake > release) was high along the reach; while for NO_3^-, the occurrence of $F_{sw} < 0$ μg N m^{-1} s^{-1} (gross uptake < release) increased along the reach. Whole-reach mass balance calculations indicated that in-stream net uptake reduced stream NH_4^+ flux up to 90%, while the stream acted mostly as a source of NO_3^- and SRP. During the dormant period, concentrations decreased along the reach for NO_3^-, but increased for NH_4^+ and SRP. During the vegetative period, NH_4^+ decreased, SRP increased, and NO_3^- showed a U-shaped pattern along the reach. These longitudinal trends resulted from the combination of hydrological mixing with terrestrial inputs and in-stream nutrient processing. Therefore, the assessment of these two sources of variation of stream water

chemistry is crucial to understand the contribution of in-stream processes to stream nutrient dynamics at relevant ecological scales.

1. Introduction

Stream water chemistry integrates hydrological and biogeochemical processes occurring within its drainage area and thus, the temporal variation of stream solute concentrations at the catchment outlet is considered a good indicator of the response of terrestrial and aquatic ecosystems to environmental drivers (Bormann and Likens, 1967; Bernhardt et al., 2003; Houlton et al., 2003). Less attention has been paid to the spatial variation of water chemistry along the stream, though it can be considerably important because stream nutrient concentrations are influenced by changes in hydrological flow paths, vegetation cover, and soil characteristics (Dent and Grimm, 1999; Likens and Buso, 2006). For instance, spatial variation in nutrient concentration along the stream has been attributed to changes in soil nitrification rates (Bohlen et al., 2001), soil organic carbon availability (Johnson et al., 2000), and organic soil depth across altitudinal gradients (Lawrence et al., 2000). Moreover, nutrient cycling within the riparian zone can strongly influence stream nutrient concentrations along the stream because these ecosystems are hot spots of biogeochemical processing (McClain et al., 2003; Vidon et al., 2010). In addition, processes occurring at the riparian-stream interface have a major influence on stream water chemistry than those occurring at catchment locations further from the stream (Ross et al., 2012). Finally, stream ecosystems have a strong capacity to transform and retain nutrients; and thus, in-stream biogeochemical processes can further influence nutrient chemistry along the stream (Peterson et al., 2001; Dent et al., 2007). Therefore, consideration of these multiple sources of variation of stream water chemistry is important to understand drivers of stream nutrient dynamics.

63 Our understanding of nutrient biogeochemistry within riparian zones and
64 streams is mainly based on field studies performed at the plot-scale or in small stream
65 reaches (few hundred meters) (Lowrance et al., 1997; Peterson et al., 2001; Sabater et
66 al., 2003; Mayer et al., 2007; von Schiller et al., 2015). These empirical studies have
67 widely demonstrated the potential of riparian and stream ecosystems as either sinks or
68 sources of nutrients, which ultimately influence the transport of nutrients to downstream
69 ecosystems. Riparian and stream biota are capable to decrease the concentration of
70 essential nutrients, such as dissolved inorganic nitrogen (DIN) and phosphate,
71 especially with increasing water storage and residence time (Valett et al., 1996; Hedin et
72 al., 1998; Peterson et al., 2001; Vidon and Hill, 2004). Conversely, riparian forests can
73 become sources rather than sinks of nutrients when N_2-fixing species predominate
74 (Helfield and Naiman, 2002; Compton et al., 2003), and in-stream nutrient release can
75 be important during some periods (Bernhardt et al., 2002; von Schiller et al., 2015).
76 Moreover, there is an intimate hydrological linkage between riparian and stream
77 ecosystems that can result in strong biogeochemical feedbacks between these two
78 compartments (e.g., Morrice et al., 1997; Martí et al., 2000; Bernal and Sabater, 2012).
79 However, studies integrating biogeochemical processes at these two nearby ecosystems
80 are rare (but see Dent et al., 2007), and the exchange of water and nutrients between
81 stream and groundwater is unknown in most studies assessing in-stream gross and net
82 nutrient uptake (Roberts and Mulholland, 2007; Covino et al., 2010; von Schiller et al.,
83 2011).

84 There is a wide body of knowledge showing the potential of riparian and stream
85 ecosystems to modify either groundwater or stream nutrient concentrations. Yet, a
86 comprehensive view of the influence of riparian and in-stream processes on stream
87 water chemistry at the catchment scale is still lacking (but see Meyer and Likens, 1979).

This gap of knowledge mostly exists because hydrological and biogeochemical processes can vary substantially along the stream (Covino and McGlynn, 2007; Jencso et al., 2010), which limits our ability to extrapolate small plot- and reach- scale measurements to larger spatial scales. Some authors have proposed that nutrient concentrations should decline along the stream if in-stream net uptake is high enough and riparian groundwater inputs are relatively small (Brookshire et al., 2009). This declining pattern is not systematically observed in reach-scale studies, which could bring us to the conclusion that terrestrial inputs are the major driver of stream water chemistry because in-stream gross uptake and release counterbalance each other most of the time (Brookshire et al., 2009). However, synoptic studies have revealed that nutrient concentrations are patchy and highly variable along the stream as a result of spatial patterns in upwelling and in-stream nutrient processing (Dent and Grimm, 1999). Thus, in-stream nutrient cycling could be substantial, but not necessarily lead to longitudinal increases or declines in nutrient concentration, a question that probably needs to be addressed at spatial scales larger than few hundred meters.

The goal of this study was to gain a better understanding of the influence of riparian groundwater inputs and in-stream biogeochemical processing on stream nutrient chemistry and fluxes in a headwater forested catchment. To approach this question, we explored the longitudinal pattern of stream nutrient (nitrate, ammonium, and phosphate) concentration along a 3.7-km reach during 1.5 years. We choose a headwater catchment as a model system to investigate drivers of spatial patterns in stream water chemistry because they typically show pronounce changes in riparian and stream features across relatively short distances (Uehlinger, 2000). First, we evaluated riparian groundwater inputs and in-stream nutrient processing as sources of variation of stream nutrient concentration along the reach. We expected stream and riparian

groundwater nutrient concentrations to be similar and strongly correlated if riparian groundwater is a major source of nutrients to the stream. In addition, we estimated the in-stream nutrient processing capacity for 14 contiguous segments along the reach with a mass balance approach. Second, we evaluated the relative contribution of riparian groundwater inputs and in-stream biogeochemical processing to stream nutrient fluxes at the whole-reach scale by applying a mass balance approach that include all hydrological input and output fluxes along the reach.

2. Study Site

The research was conducted in the Font del Regàs catchment (14.2 km^2) (Figure 1), located in the Montseny Natural Park, NE Spain (41º50'N, 2º30'E, 300-1200 m a.s.l.) during the period 2010-2011. Total inorganic N deposition in this area oscillates between 15-30 kg N ha^{-1} $year^{-1}$ (Àvila and Rodà 2012). The climate at the Montseny Mountains is subhumid Mediterranean. The long-term mean annual precipitation is 925±151 mm and the long-term mean annual air temperature is 12.1±2.5 ºC (mean ± SD, period: 1940-2000, Catalan Metereologic Service: http://www.meteo.cat/servmet/index.html). During the study period, mean annual precipitation (975 mm) and temperature (12.9 ºC) fall within the long-term average (data from a meteorological station within the study catchment). In this period, summer was the driest season (140 mm) while most of the precipitation occurred in winter 2010 (370 mm) and autumn 2011 (555 mm) (Figure 2a).

The catchment is dominated by biotitic granite (ICC, 2010) and it has steep slopes (28%). Evergreen oak (*Quercus ilex*) and beech (*Fagus sylvatica*) forests cover 54% and 38% of the catchment area, respectively (Figure 1). The upper part of the catchment (2%) is covered by heathlands and grasslands (ICC, 2010). The catchment has a low population density (< 1 person km^{-2}) which is concentrated in the valley

138 bottom. Hillslope soils (pH ~ 6) are sandy, with high content of rocks (33-36%). Soils at
139 the hillslopes have a 3-cm depth O-horizon and a 5- to 15-cm depth A-horizon
140 (averaged from 10 soil profiles).

141 The riparian zone is relatively flat (slope < 10%), and it covers 6% of the
142 catchment area. Riparian soils (pH ~ 7) are sandy-loam with low rock content (13%)
143 and a 5-cm depth organic layer followed by a 30-cm depth A-horizon (averaged from 5
144 soil profiles). Along the 3.7-km reach, the width of the riparian zone increases from 6 to
145 32 m, whereas the total basal area of riparian trees increases by 12 folds (based on forest
146 inventories of 30-m plots every ca. 150 m) (Figure S1). *Alnus glutinosa*, *Robinia*
147 *pseudoacacia*, *Platanus hybrida*, and *Fraxinus excelsior* are the most abundant riparian
148 tree species followed by *Corylus avellana*, *Populus tremula*, *Populus nigra*, and
149 *Sambucus nigra*. The abundance of N_2-fixing species (*A. glutinosa* and *R.*
150 *pseudoacacia*) increases from 0% to > 60% along the longitudinal profile, (Figure S1).
151 During base flow conditions, riparian groundwater (< 1.5 m from the stream channel)
152 flows well below the soil surface (0.5 ± 0.1 m) and thus, the interaction with the riparian
153 organic soil is minimal (averaged from 15 piezometers, n = 165) (Figure S1). During
154 the period of study, riparian groundwater temperature ranged from 5 to 19.5 ºC.

155 The 3.7-km study reach is a 2^{nd} order stream along the first 1.5 km and a 3^{rd}
156 order stream for the remaining 63% of its length. The geomorphology of the stream bed
157 changes substantially with stream order. The stream bed along the 2^{nd} order section is
158 mainly composed of rocks and cobbles (70%) with a small contribution of sand (~
159 10%). At the valley bottom, sands and gravels represent 44% of the stream substrate
160 and the presence of rocks is minor (14%). Mean wetted width and water velocity
161 increase between the 2^{nd} and 3^{rd} order section (from 1.6 to 2.7 m and from 0.24 to 0.35
162 m s^{-1}, respectively) (Figure S1). During the study period, stream water temperature

163 ranged from 5 to 18ºC. Stream discharge was low in summer (0.33 mm) and peaked in
164 spring (0.79 mm).

165 **3. Materials and Methods**

166 *3.1. Field sampling and laboratory analysis*

167 We selected 15 sampling sites along the 3.7-km study reach. The distance
168 between consecutive sampling sites ranged from 110 to 600 m (Figure 1). At each
169 sampling site, we installed a 1-m long PVC piezometer (3-cm Ø) in the riparian zone at
170 ~ 1.5 m from the stream channel.

171 For each sampling site, we sampled stream water (from the thalweg) and riparian
172 groundwater every 2 months from August 2010 to December 2011. We used pre-acid
173 washed polyethylene bottles to collect water samples after triple-rinsing them with
174 either stream or groundwater. On each sampling date, we also measured dissolved
175 oxygen concentration (DO, in mg l^{-1}) and water temperature (T, in ºC) with an YSI
176 ProODO device in both stream water and in riparian groundwater. We avoid sampling
177 soon after storms to ensure that our measurements were representative of low flow
178 conditions, when the influence of in-stream biogeochemical processes on stream
179 nutrient concentrations and fluxes is expected to be the highest. All field campaigns
180 were performed at least 9 days after storm events, except in October 2011 (Figure 2b,
181 black squares). On each sampling date and at each sampling site, we measured
182 groundwater table elevation (in m below soil surface) with a water level sensor
183 (Eijkelkamp 11.03.30) as well as wetted width (in m), stream discharge (Q, in l s^{-1}), and
184 water velocity (m s^{-1}). Q and water velocity were estimated with the slug-addition
185 technique by adding 1 l of NaCl-enriched solution to the stream (electrical conductivity
186 = 75-90 mS cm^{-1}, n = 11) (Gordon et al., 2004). The uncertainty associated with Q
187 measurements was calculated as the relative difference in Q between pairs of tracer

188 additions under equal water depth conditions (difference < 1 mm). The pairs of data
189 were selected from a set of 126 slug additions and water level measurements obtained
190 from the permanent field stations at Font del Regàs (Lupon, unpublished). The
191 measured uncertainty was relatively small (1.9%, n = 11). On each sampling date, we
192 also collected stream water and measured *Q* at the four permanent tributaries
193 discharging to Font del Regàs stream, which drained 1.9, 3.2, 1.8, and 1.1 km^2,
194 respectively (Figure 1). These data were used for mass balance calculations (see below).
195 Additional stream water samples were collected from a small permanent tributary that
196 drained through an area (< 0.4 km^2) with few residences and crop fields for personal
197 consumption.

198 Water samples were filtered through pre-ashed GF/F filters (Whatman®) and
199 kept cold (< 4ºC) until laboratory analysis (< 24h after collection). Chloride (Cl^-) was
200 used as a conservative hydrological tracer and analyzed by ionic chromatography
201 (Compact IC-761, Methrom). Nitrate (NO_3^-) was analyzed by the cadmium reduction
202 method (Keeney and Nelson 1982) using a Technicon Autoanalyzer (Technicon, 1976).
203 Ammonium (NH_4^+) was manually analyzed by the salicilate-nitropruside method
204 (Baethgen and Alley 1989) using a spectrophotometer (PharmaSpec UV-1700
205 SHIMADZU). Soluble reactive phosphorus (SRP) was manually analyzed by the acidic
206 molybdate method (Murphy and Riley, 1962) using a spectrophotometer (PharmaSpec
207 UV-1700 SHIMADZU).

208 *3.2. Data analysis*

209 The seasonality of biological activity can strongly affect both riparian
210 groundwater chemistry and in-stream biogeochemical processes (Groffman et al., 1992;
211 Hill et al., 2001). Therefore, the data set was separated in two groups based on sampling
212 dates during the vegetative and dormant period (7 and 4 sampling dates, respectively).

As a reference, we considered the vegetative period starting at the beginning of riparian leave out (April) and ending at the peak of leave-litter fall (October), coinciding with the onset and offset of riparian tree evapotranspiration, respectively (Nadal-Sala et al., 2013). During the study period, rainfall was similar between the vegetative and dormant period (775 and 876 mm, respectively).

3.2.1. Patterns of stream discharge, riparian groundwater inputs, and stream solute concentrations

For each period, we examined the longitudinal pattern of stream discharge, riparian groundwater inputs, and stream solute concentrations along the reach. On each sampling date, we calculated area-specific stream discharge by dividing instantaneous discharge by catchment area (Q', in mm d^{-1}) at each sampling site. We used Q' rather than Q to be able to compare water fluxes from the 15 nested catchments along the reach. We examined the longitudinal patterns of Q' and stream solute concentration (C_{sw}) by applying regression models (linear, exponential, potential, and logarithmic). Model selection was performed by ordinary least square (Zar, 2010). We referred only to the best fit model in each case.

The contribution of net riparian groundwater inputs to surface water along each stream segment (Q_{gw}) was estimated as the difference in Q between consecutive sampling sites (Covino et al., 2010). The empirical uncertainty associated with Q was used to calculate a lower and upper limit of Q_{gw}. We considered that Q_{gw} was representative of the net riparian groundwater flux draining to the stream within each stream segment. We acknowledge that this approach oversimplifies the complex hydrological interactions at the riparian-stream interface because it does not consider concurrent hydrological gains and losses within each segment (Payn et al., 2009), but

238 we consider that it provides a representative estimate at the scale of this study. To
239 investigate the longitudinal pattern of riparian groundwater inputs, we calculated the
240 cumulative area-specific net riparian groundwater input ($\Sigma Q'_{gw}$, in mm d^{-1}) by summing
241 up Q_{gw} from the upstream-most site to each of the downstream segments and dividing it
242 by the cumulative catchment area.

243 For each sampling date, we examined whether the 3.7-km reach was either net
244 gaining or net losing water by comparing concurrent gross hydrological gains and losses
245 over the entire reach (Payn et al., 2009). For this spatial scale, we considered that stream
246 segments exhibiting $Q_{gw} > 0$ contributed to gross hydrological gains ($\Sigma Q_{gw} > 0$) while
247 segments with $Q_{gw} < 0$ contributed to gross hydrological losses ($\Sigma Q_{gw} < 0$). Note that
248 gross riparian groundwater fluxes divided by the total catchment area are equal to $\Sigma Q'_{gw}$
249 at the downstream-most site. For each sampling date, we calculated the relative
250 contribution of different water sources to stream discharge at the downstream-most site
251 (Q_{bot}), with Q_{top}/Q_{bot}, $\Sigma Q_{ef}/Q_{bot}$, and $\Sigma Q_{gw}/Q_{bot}$ for upstream, tributaries and riparian
252 groundwater, respectively.

253

254 *3.2.2. Sources of variation of stream nutrient concentration along the reach*

255 *Riparian groundwater inputs.* We investigated whether longitudinal patterns in
256 stream solute concentration were driven by riparian groundwater inputs by comparing
257 solute concentrations between stream water and riparian groundwater with a Wilcoxon
258 paired sum rank test. A non-parametric test was used because solute concentrations
259 were not normally distributed (Shapiro-Wilk test, $p < 0.01$ for all study solutes) (Zar,
260 2010).

261 Moreover, we examined the degree of hydrological interaction at the riparian-
262 stream interface by exploring the relationship between stream and riparian groundwater

263 Cl^- concentrations with a Spearman correlation. For each period, we quantified the
264 difference between Cl^- concentrations in the two water bodies by calculating
265 divergences from the 1:1 line with the relative root mean square error (RRMSE, in %):

266 $$RRMSE = \frac{\sqrt{\sum_{i=1}^{n}\left(C_{sw} - C_{gw}\right)^2}}{n \cdot \overline{C_{gw}}} \cdot 100 \quad (1)$$

267 where C_{sw} and C_{gw} are stream and riparian groundwater solute concentrations,
268 respectively, n is the total number of observations, and $\overline{C_{gw}}$ is the average of C_{gw}. A
269 strong correlation and a low RRMSE between stream and riparian groundwater Cl^-
270 concentrations indicate a strong hydrological connection between the two water bodies.
271 Similarly, we examined the correlation between stream and riparian groundwater
272 nutrient concentrations. We expected a weak correlation and a high RRMSE value
273 between nutrient concentrations measured at the two water bodies if the stream has a
274 high nutrient processing capacity and in-stream gross uptake and release do not
275 counterbalance each other.

276 *In-stream nutrient processing*. We investigated the influence of in-stream
277 biogeochemical processes on the longitudinal pattern of stream nutrient concentrations
278 by applying a mass balance approach for each individual segment (Roberts and
279 Mulholland, 2007). For each nutrient, we calculated changes in stream flux between
280 contiguous sampling sites (F_{sw}, in μg m^{-1} s^{-1}), being F_{sw} the net flux resulting from in-
281 stream gross uptake and release along a particular stream segment (von Schiller et al.,
282 2011). We expressed F_{sw} by unit of stream length in order to compare net changes in
283 stream flux between segments differing in length. For each sampling date and for each
284 nutrient, F_{sw} was approximated with:

285 $$F_{sw} = (F_{top} + F_{ef} + F_{gw} - F_{bot})/\, x, \quad (2)$$

where F_{top} and F_{bot}, are the nutrient flux at the top and at the bottom of each stream segment, F_{gw} is the nutrient flux from net riparian groundwater inputs, and F_{ef} is the nutrient flux from effluent inputs for those reaches including a tributary (all in $\mu g\ s^{-1}$) (Figure 3). F_{top} and F_{bot} were calculated by multiplying Q by C_{sw} at the top and at the bottom of the segment, respectively. F_{gw} was estimated by multiplying net groundwater inputs (Q_{gw}) by nutrient concentration in either riparian groundwater or stream water. For net gaining segments ($Q_{gw} > 0$), we assumed that the chemistry of net water inputs was similar to that measured in riparian groundwater and thus, C_{gw} was the average between riparian groundwater nutrient concentration at the top and bottom of the reach. For net losing segments ($Q_{gw} < 0$), we assumed that the chemistry of net water losses was similar to that measured in stream water and thus, C_{gw} averaged stream water concentration at the top and at the bottom of each reach segment (C_{top} and C_{bot}, respectively). For those cases in which stream segments received water from a tributary, F_{ef} was calculated by multiplying Q and C at the outlet of the tributary. We calculated an upper and lower limit of F_{sw} based on the empirical uncertainty associated with water fluxes (Q and Q_{gw}). Finally, x (in m) is the length of the segment between two consecutive sampling sites. The same approach was applied for Cl^-, a conservative tracer that was used as a hydrological reference. For Cl^-, we expected $F_{sw} \sim 0$ if inputs from upstream, tributaries, and riparian groundwater account for most of the stream Cl^- flux. For nutrients, F_{sw} can be positive (gross uptake > release), negative (gross uptake < release) or nil (gross uptake ~ release). Therefore, we expected $F_{sw} \neq 0$ if in-stream gross uptake and release processes do not fully counterbalance each other (von Schiller et al., 2011). To investigate whether stream segments were consistently acting as net sinks or net sources of nutrients along the stream during the study period, we calculated the frequency of $F_{sw} > 0$, $F_{sw} < 0$, and $F_{sw} = 0$ for each nutrient and for each segment..

We assumed that F_{sw} was undistinguishable from 0 when its upper and lower limit contained zero.

Since in-stream nutrient cycling can substantially vary with reach length (Meyer and Likens, 1979; Ensign and Doyle, 2006), we also calculated F_{sw} for the whole 3.7-km reach by including all hydrological input and output fluxes (solute fluxes from the upstream-most site, tributaries, and riparian groundwater gross gains and losses) in a mass balance at the whole-reach scale. For the two spatial scales (segment and whole reach), we examined whether F_{sw} differed among nutrients with a Mann Whitney test.

3.2.3. Relative contribution of riparian groundwater and in-stream nutrient processing to stream nutrient fluxes

To assess the relevance of F_{sw} compared to input solute fluxes, we calculated the ratio between $F_{sw} \cdot x$ (absolute value) and the total input flux (F_{in}) for each solute and sampling date. For the two spatial scales (segment and whole reach), F_{in} was the sum of upstream (F_{top}), tributaries (F_{ef}), and net riparian groundwater inputs (F_{gw}). The latter was included when $Q_{gw} > 0$. We interpreted a high $|F_{sw} \cdot x / F_{in}|$ ratio as a strong potential of in-stream processes to modify input fluxes (either as a consequence of gross uptake or release). For each spatial scale, we explored whether $|F_{sw} \cdot x / F_{in}|$ differed among nutrients with a Mann Whitney test.

We used a whole-reach mass balance approach to assess the relative contribution of net riparian groundwater inputs ($F_{gw} > 0 / F_{in}$) and in-stream release ($|F_{sw} < 0 / F_{in}|$) to stream solute fluxes. In addition, we calculated the contribution of upstream (F_{top}/F_{in}) and tributary inputs (F_{ef}/F_{in}) to stream solute fluxes. For each solute, we analyzed differences in the relative contribution of different sources to stream input fluxes with a Mann Whitney test. Finally, when the whole reach was acting as a net sink for a

particular nutrient ($F_{sw} > 0$), we calculated the relative contribution of in-stream net uptake to reduce stream nutrient fluxes along the 3.7-km reach with $F_{sw} \cdot x / F_{in}$.

4. Results

4.1. Hydrological characterization of the stream reach

During the study period, mean Q' decreased from 0.82 ± 0.13 [mean ± SE] to 0.54 ± 0.11 mm d^{-1} along the reach (linear regression [l.reg], $r^2 = 0.79$, degrees of freedom [df] = 14, F = 51.4, $p < 0.0001$) (Figure 4a). This pattern hold for the two seasonal periods considered (dormant and vegetative; Wilcoxon rank sum test, $p > 0.05$).

On average, the stream was net gaining water along the 3.7-km reach, though the hydrological interaction between the riparian zone and the stream was highly variable across contiguous segments (Figure 4b). The stream was consistently gaining water along the first 1.5 km and the last 0.5 km, while hydrological losses were evident along the intermediate 2 km (Figure 4b). At the whole-reach scale, gross hydrological gains exceed gross losses in 8 out of 10 field dates (Figure 2c and d). This was especially noticeable in April and December 2011, the two sampling dates most influenced by storm events. In contrast, the whole reach was acting as net hydrological losing in March and October 2011.

Stream Cl^- concentrations showed a 40% increase along the reach (l.reg, $r^2 = 0.88$, df = 14, F = 44.6, $p < 0.0001$), which contrasted with the longitudinal pattern exhibited by stream discharge (Figure 4c). The two periods showed a similar longitudinal pattern, though stream Cl^- concentration was lower during the dormant than during the vegetative period (Wilcoxon rank sum test, Z = -6.4, $p < 0.0001$) (Table 1). The same seasonal pattern was exhibited by the five permanent tributaries (Figure 4c).

360 There was a strong correlation between stream and riparian groundwater Cl^-
361 concentrations, which fitted well to the 1:1 line (low RRMSE for the two periods)
362 (Table 2 and Figure S2).

363 The mean net change in Cl^- flux within individual segments was 0.4 ± 0.03 mg
364 m^{-1} s^{-1}, which represented a small fraction of the Cl^- input flux ($|F_{sw} \cdot x / F_{in}| < 6$ %).
365 Similar results were obtained when calculating Cl^- budgets for the whole-reach
366 approach (Table 3). The stream Cl^- flux was mainly explained by inputs from tributaries
367 followed by riparian groundwater and upstream (Table 4). Similar results were obtained
368 when calculating the relative contribution of different water sources to stream discharge
369 at the whole-reach scale.

370 *4.2. Longitudinal pattern of stream nutrient concentration*

371 The longitudinal pattern of stream concentration differed between nutrients and
372 periods. During the dormant period, stream NO_3^- concentration decreased along the
373 reach especially within the first 1.5 km (l.reg, $r^2 = 0.47$, df = 15, F = 11.4, $p < 0.005$)
374 (Figure 5a). During the vegetative period, stream NO_3^- concentration showed a U-
375 shaped pattern: it decreased along the first 1.5 km, remained constant along the
376 following 1 km, and increased by 60% along the last km of the reach (Figure 5a).
377 Despite these differences, stream NO_3^- concentration was similar between the dormant
378 and vegetative period for both the main stream and tributaries (in all cases, Wilcoxon
379 rank sum test, $p > 0.05$) (Table 1).

380 Stream NH_4^+ concentration showed an increasing longitudinal pattern during the
381 dormant period (exponential regression [e.reg], $r^2 = 0.45$, df = 15, F = 10.5, $p < 0.01$),
382 while concentration decreased during the vegetative period (logarithmic regression
383 [lg.reg], $r^2 = 0.42$, df = 15, F = 9.6, $p < 0.01$) (Figure 5b). The main stream showed

384 higher NH_4^+ concentration during the vegetative than during the dormant period
385 (Wilcoxon rank sum test, $Z_{NH4} = -3.5$, $p < 0.001$) (Table 1). For the tributaries, NH_4^+
386 concentration was similar between the two periods (in all cases, Wilcoxon rank sum
387 test, $p > 0.01$).

388 Stream SRP concentration increased along the reach during both the dormant
389 (e.reg, $r^2 = 0.59$, $F = 18.5$, $df = 14$, $p < 0.01$) and vegetative period (l.reg, $r^2 = 0.49$, $F =$
390 12.4, $df = 14$, $p < 0.01$) (Figure 5c). Similarly to NH_4^+, the main stream showed higher
391 SRP concentration during the vegetative than during the dormant period (Wilcoxon rank
392 sum test, $Z_{SRP} = -6.6$, $p < 0.001$) (Table 1). For the tributaries, SRP concentration was
393 similar between the two periods (in all cases, Wilcoxon rank sum test, $p > 0.01$).

394 *4.3. Sources of variation of stream nutrient concentration*

395 *Riparian groundwater inputs.* The relationship between stream and riparian
396 groundwater concentrations differed between nutrients and periods. During the dormant
397 period, stream and riparian groundwater NO_3^- concentrations were similar, while the
398 stream showed higher concentration during the vegetative period (Table 1). During the
399 two periods, stream and riparian groundwater NO_3^- concentrations were positively
400 correlated and showed relatively small RRMSE (Table 2 and Figure S2). NH_4^+
401 concentration in stream water was 2-3 folds lower than in riparian groundwater (Table
402 1), and stream and groundwater concentrations were no correlated either during the
403 dormant or vegetative periods (Table 2). Stream and riparian groundwater SRP
404 concentrations were similar in the two periods (Table 1). During the dormant period,
405 SRP concentration showed a significant correlation between the two water bodies, while
406 no correlation and relatively high RRMSE occurred during the vegetative period (Table
407 2). The differences in nutrient concentrations between stream and riparian groundwater

408 in the two study periods were accompanied by consistently higher DO concentrations in
409 the stream than in riparian groundwater (Table 1).

410 *In-stream nutrient processing*. The influence of in-stream nutrient processing on
411 stream water chemistry differed among nutrients. During the study period, median F_{sw}
412 was negative for NO_3^-, positive for NH_4^+, and close to 0 for SRP (Table 3). Yet,
413 differences in F_{sw} were not statistically significant among nutrients for either the
414 vegetative or dormant period (for both periods: Mann Whitney test with post-hoc Tukey
415 test, $p > 0.05$). Similar F_{sw} values were obtained when calculating nutrient budgets
416 either by segment or whole reach (Table 3).

417 The frequency of an individual segment to act either as a nutrient sinks or source
418 differed among nutrients and along the reach. For NO_3^-, the frequency of $F_{sw,NO3} < 0$
419 (gross uptake < release) increased from 9 to > 50% along the reach (l.reg, $r^2 = 0.55$, df =
420 13, $F = 14.67$, $p < 0.01$) (Figure 6a). For NH_4^+, the frequency of $F_{sw,NH4} > 0$ (gross
421 uptake > release) was high across individual segments, ranging from 20 to 90% (Figure
422 6b). For SRP, the frequency of $F_{sw,SRP} < 0$, > 0, or ~ 0 did not show any consistent
423 longitudinal pattern (Figure 6c). Overall, the frequency of sampling dates for which in-
424 stream biogeochemical processes were imbalanced ($F_{sw} \neq 0$) was lower for NO_3^- (36%)
425 than for NH_4^+ (80%) and SRP (68%) (Figure 6).

426 *4.4. Relative contribution of riparian groundwater and in-stream processing to stream*
427 *nutrient fluxes at the segment and whole-reach scale*

428 The capacity of in-stream processes to modify stream input fluxes differed
429 between nutrients and spatial scales. For individual segments, $|F_{sw} \cdot x / F_{in}|$ was smaller for
430 NO_3^- (6%) than for NH_4^+ and SRP (~20%) (Mann Whitney test with post-hoc Tukey

431 test, $p < 0.01$, Table 3). However, $|F_{sw} \cdot x/F_{in}|$ increased substantially for NO_3^- and NH_4^+
432 when nutrient budgets were calculated at the whole-reach scale (Table 3).

433 According to whole-reach mass balance calculations, the stream acted as a net
434 source of NO_3^- on 7 out of the10 sampling dates for which whole-reach budgets were
435 calculated. The contribution of in-stream release to stream NO_3^- fluxes was as important
436 as that of riparian groundwater and upstream fluxes (Table 4). In-stream net NO_3^-
437 retention at the whole-reach scale was observed only in spring (March and April 2011)
438 (Figure 7a).

439 In contrast to NO_3^-, the stream consistently acted as a net sink of NH_4^+ and it
440 retained up to 90% of the input fluxes in spring and autumn (Figure 7b). The stream
441 acted as a source of NH_4^+ in summer (Figure 7b), though the contribution of in-stream
442 release to stream NH_4^+ fluxes was minimal compared to that from riparian groundwater
443 (Table 4).

444 The stream acted as a net source of SRP in 6 out of the 10 sampling dates. The
445 contribution of in-stream release to stream SRP fluxes was as important as that of
446 riparian groundwater (Table 4). In-stream net SRP retention was minimal, except in
447 autumn 2011 (October and December 2011) (Figure 7c).

448 **5. Discussion**

449 In terms of hydrology, the study headwater stream was a net gaining reach,
450 though the hydrological interaction between the riparian zone and the stream was
451 complex as indicated by the longitudinal variation in net riparian groundwater inputs.
452 Moreover, the longitudinal decrease in area-specific discharge suggests that
453 hydrological retention increased at the valley bottom compared to upstream segments as
454 reported in previous studies (Covino et al., 2010). Despite the complex hydrological

455 processes along the reach, the strong positive correlation between stream and riparian
456 groundwater Cl^- concentration suggests high hydrological connectivity at the riparian-
457 stream interface (Butturini et al., 2003). In addition, we found that the permanent
458 tributaries, which comprised ~ 50% of the catchment area, contributed 56% of stream
459 discharge; and thus, they were an essential piece to understand stream nutrient
460 chemistry and loads. Hydrological mixing of stream water with water from tributaries
461 could partially explain the longitudinal increase in Cl^- because its concentration was
462 higher at the tributaries than at the main stream, especially during the vegetative period.
463 In addition, riparian groundwater inputs to the stream could further contribute to the
464 longitudinal increase in stream Cl^- concentration because they contributed 26% of
465 stream discharge and also exhibited higher Cl^- concentration than stream water.

466 Based on the strong hydrological connectivity between the stream and the
467 riparian groundwater and the large contribution of tributaries to stream discharge, one
468 would expect a strong influence of these water sources on the longitudinal variation of
469 stream nutrient chemistry. However, the relationship between stream and riparian
470 groundwater nutrient concentration was from moderate to weak for NO_3^- and SRP, and
471 nil for NH_4^+. Further, the contribution of tributaries to stream nutrient fluxes was
472 relatively small (from 21 to 34%) compared to their contribution to stream Cl^- and water
473 fluxes (> 50%). Together these data suggest that longitudinal patterns of stream nutrient
474 concentration could not be explained by hydrological mixing alone; and thus, pointed at
475 in-stream biogeochemical processing as a likely mechanism to modify nutrient
476 concentrations along the study reach. In fact, the estimates of in-stream net nutrient
477 uptake (F_{sw}) at the different stream segments supported this idea and agreed with
478 previous studies showing that in-stream processes can mediate stream nutrient

chemistry and downstream nutrient export (McClain et al., 2003; Harms and Grimm, 2008).

Our results revealed an extremely high variability in F_{sw}, that could range up to one order of magnitude, across individual segments and over time, which agrees with findings from other headwater streams (von Schiller et al., 2011). However, some general trends aroused when comparing patterns for the different studied nutrients. For instance, the frequency of dates for which in-stream gross uptake and release were imbalanced ($F_{sw} \neq 0$) was higher for NH_4^+ (80%) and SRP (68%) than for NO_3^- (37%). Further, the potential of in-stream processes to modify stream fluxes within stream segments ($|F_{sw} \cdot x/F_{in}|$) was 3 folds higher for NH_4^+ and SRP than for NO_3^-. Our findings are concordant with studies performed at short stream reaches (< 300 m) worldwide, which show that in-stream gross uptake velocity (as a proxy of nutrient demand) is typically higher for NH_4^+ and SRP than for NO_3^- (Ensign and Doyle, 2006). This difference among nutrients is commonly attributed to the higher biological demand for NH_4^+ and SRP than for NO_3^-. However, we found that F_{sw} was similar among nutrients; and thus, differences in $|F_{sw} \cdot x/F_{in}|$ were mainly associated with differences in the concentration of the inputs, which tend to be 20 folds lower for NH_4^+ and SRP than for NO_3^-. Divergences between F_{sw} and $|F_{sw} \cdot x/F_{in}|$ were even more remarkable when nutrient budgets were considered at the whole-reach scale, especially for DIN forms. NO_3^- and NH_4^+ showed no differences in F_{sw} between the two scales of observation; however, they showed a substantial increase in $|F_{sw} \cdot x/F_{in}|$ at the whole-reach scale (length of kilometers) compared to the segment scale (length of hundreds of meters). Similarly, previous nutrient spiraling studies have reported an increase in the proportion of nutrient removal with stream order despite no changes in gross uptake rates among stream reaches (Ensign and Doyle, 2006; Wollheim et al., 2006). This pattern has been

attributed to variation in intrinsic stream characteristics, such as stream nutrient concentration, discharge, stream width, and the size of the hyporheic zone (Wollheim et al., 2006; Alexander et al., 2009), which may also hold for our study since these characteristics varied along the 3.7-km reach. However, our results also indicate that the assessment of riparian groundwater inputs is crucial to understand the contribution of in-stream processes to stream nutrient fluxes. Overall, our findings add to the growing evidence that streams are hot spots of nutrient processing (Peterson et al., 2001; Dent et al., 2007), and that in-stream processes can substantially modify stream nutrient fluxes at the catchment scale (Ensign and Doyle, 2006; Bernal et al., 2012).

The potential of in-stream processes to regulate stream nutrient fluxes was especially remarkable for NH_4^+. There was no relationship between stream and riparian groundwater NH_4^+ concentrations; and further, whole-reach budgets indicated that in-stream net uptake could reduce the flux of NH_4^+ up to 90% along the reach. This high in-stream bioreactive capacity could be favored by the sharp increase in redox conditions from riparian groundwater to stream water (Hill et al., 1998; Dent et al., 2007). Concordantly, NH_4^+ concentrations were higher in riparian groundwater than in the stream, while the opposite occurred for NO_3^- (although only during the vegetative period). These results suggest fast nitrification of groundwater inputs within the stream as environmental conditions become well oxygenated (Jones et al., 1995). Supporting this idea, we found that in-stream gross NH_4^+ uptake prevailed over release along the reach. However, the marked increase in stream NO_3^- concentration observed along the last 700 m of the reach during the vegetative period could not only be explained by nitrification of riparian groundwater NH_4^+ because this flux ($F_{gw,NH4} \sim 2$ μg N m^{-1} s^{-1}) was not large enough to sustain in-stream NO_3^- release ($|F_{sw,NO3} < 0|$ (~ 10 μg N m^{-1} s^{-1}). This finding suggests an additional source of N at the valley bottom. Previous studies

529 have shown that leaf litter from riparian trees, and especially from N_2-fixing species,
530 can enhance in-stream nutrient cycling because of its high quality and edibility (Starry
531 et al., 2005; Mineau et al., 2011). Thus, the increase in NO_3^- and SRP concentrations
532 and in-stream NO_3^- release observed at the lowest part of the catchment during the
533 vegetative period could result from the combination of warmer temperatures and the
534 mineralization of large stocks of alder and black locust leaf litter stored in the stream
535 bed (Strauss and Lamberti, 2000; Bernhardt et al., 2002; Starry et al., 2005).
536 Alternatively, increases in stream NO_3^- and SRP concentration could result from human
537 activities, which were concentrated at the lowest part of the catchment. However,
538 regarding NO_3^-, anthropogenic sources seem unlikely because DIN concentrations at the
539 tributary draining through the inhabited area were low. In contrast, this tributary showed
540 high SRP concentrations (from 2 to 6 folds higher than in the main stream), though its
541 discharge should have had to be ca. 4 times higher than expected for its drainage area (<
542 0.4 km^2) to explain the observed changes in concentration. Another possible explanation
543 for the increase in stream N concentration at the valley bottom could be increased N
544 fixation by stream algae (Finlay et al., 2011). However, in-stream DIN release (NO_3^-
545 and NH_4^+) peaked in late spring and summer (May and August 2011), when light
546 penetration was limited by riparian canopy and in-stream photoautotrophic activity was
547 low (Lupon et al., 2014). Altogether, these data suggest that the sharp increase in
548 nutrient availability along the last 700 m of the reach was likely related to the massive
549 presence of the invasive black locust at the valley bottom. Black locust is becoming
550 widespread throughout riparian floodplains in the Iberian Peninsula (Castro-Díez et al.,
551 2014) and its potential to subsidize N to stream ecosystems via root exudates and leaf
552 litter could dramatically alter in-stream nutrient processing and downstream nutrient
553 export (e.g., Stock et al., 1995; Mineau et al., 2011). However, further research is

554 needed to test the hypothesis that this invasive species can alter stream nutrient
555 dynamics in riparian floodplains.

556 It is worth noting that longitudinal trends in stream nutrient concentration were
557 not always pointing towards the same direction than estimates based on in-stream
558 processes. This divergence evidenced that other sources of variation of stream water
559 chemistry were counterbalancing the influence of in-stream processes on stream nutrient
560 fluxes. In this sense, results from NH_4^+ were paradigmatic. The mass balance approach
561 clearly showed that in-stream gross uptake of NH_4^+ exceeded release; and concordantly,
562 NH_4^+ concentration was consistently lower in the stream than in riparian groundwater.
563 Yet, stream NH_4^+ concentration showed small longitudinal variation likely because in-
564 stream net uptake balanced the elevated inputs from riparian groundwater. Therefore,
565 our results challenge the idea that stream nutrient concentration should decrease in the
566 downstream direction when in-stream processes are efficient in taking up nutrients from
567 receiving waters (Brookshire et al., 2009). Conversely, our findings convincingly show
568 that in-stream processes can strongly affect stream nutrient chemistry and downstream
569 nutrient export despite this may not result in consistent longitudinal gradients in nutrient
570 concentration. For NO_3^-, we found that the marked increase in concentration along the
571 last 700 m could be attributed to an increase in in-stream nitrification. However, the
572 observed decrease in NO_3^- concentration along the first 1.5 km of the reach could be
573 barely explained by in-stream processing alone because its contribution to reduce
574 stream NO_3^- fluxes was too low, even when the whole-reach budget was recalculated
575 excluding the last 700 m of the reach (F_{sw} = 0.61 μg N m^{-1} s^{-1} and $F_{sw} > 0/F_{in}$ = 10%).
576 For SRP, the longitudinal increase in concentration could neither be fully explained by
577 in-stream release because $F_{sw,SRP} < 0$ was not widespread along the reach and the stream
578 only contributed to input fluxes by 19% (6% when excluding the last 700 m). In fact,

579 our whole-reach mass balance indicated that stream nutrient chemistry along the reach
580 resulted from the combination of both in-stream nutrient processing and hydrological
581 mixing with riparian groundwater and tributary inputs. Recent studies have concluded
582 that riparian groundwater is a major driver of longitudinal patterns in stream nutrient
583 concentration in headwater streams (Bernhardt et al., 2002; Asano et al., 2009; Scanlon
584 et al., 2010). Our study adds to our knowledge of catchment biogeochemistry by
585 showing that stream nutrient chemistry results from the combination of both
586 hydrological mixing from the riparian zone and in-stream nutrient processing, which
587 can play a pivotal role on shaping stream nutrient concentrations and fluxes at the
588 catchment scale.

589 **6. Conclusions**

590 The synoptic approach adopted in this study highlighted that the Font del Regàs
591 stream had a strong potential to transform nutrients. Longitudinal pattern in stream
592 nutrient concentrations could not be explained solely by hydrological mixing with
593 riparian groundwater and tributary sources because dissolved nutrients underwent
594 biogeochemical transformation while travelling along the stream channel. Our results
595 revealed that in-stream processes were highly variable over time and space, though in
596 most cases this variability could not be associated with either physical longitudinal
597 gradients or shifts in environmental conditions between the dormant and vegetative
598 period. Nevertheless, results from a mass balance approach showed that in-stream
599 processes contributed substantially to modify stream nutrient fluxes and that the stream
600 could act either as a net nutrient sink (for NH_4^+) or as a net nutrient source (for SRP and
601 NO_3^-) at the catchment scale. These results add to the growing evidence that in-stream
602 biogeochemical processes may be taken into consideration in either empirical or

603 modeling approaches if we are to understand drivers of stream nutrient chemistry within
604 catchments.

605 Recent studies have proposed that riparian groundwater is a major control of
606 longitudinal patterns of nutrient concentration because in-stream gross nutrient uptake
607 and release tend to counterbalance each other most of the time (Brookshire et al., 2009;
608 Scanlon et al., 2010). Conversely, our study showed that in-stream processes can
609 influence stream nutrient chemistry and downstream exports without generating
610 longitudinal gradients in concentration and flux because changes in stream nutrient
611 chemistry are the combination of both in-stream processing and nutrient inputs from
612 terrestrial sources. Our results imply that the assessment of these two sources of
613 variation of stream nutrient chemistry is crucial to understand the contribution of in-
614 stream processes to stream nutrient dynamics at relevant ecological scales.

615 Reliable measurements of riparian groundwater inputs are difficult to obtain
616 because spatial variability can be high (Lewis et al., 2006) and to determine the
617 chemical signature of the groundwater that really enters the stream is still a great
618 challenge (Brookshire et al., 2009). In this study, we installed 15 piezometers along the
619 reach (one per sampling site) which may not be representative enough of the variation
620 of riparian groundwater chemistry. However, and despite its limitations, riparian
621 groundwater sampling near the stream can help to constrain the uncertainty associated
622 with this water source and provide more reliable estimations of in-stream net nutrient
623 uptake for both nutrient mass balance and spiraling empirical approaches (von Schiller
624 et al., 2011).

Author contribution

S.B., F.S., and E.M. designed the experiment. S.B, A.L., M.R., and F.S. carried them out. A.L. performed all laboratory analysis. S.B. analyzed the data set and prepared the manuscript with contributions from A.L., M.R., and E.M.

Aknowledgements

We thank A. Oltra for assisting with GIS, and S. Poblador, E. Martín, and C. Romero for field assistance. S.B. and A.L. were funded by the Spanish Ministry of Economy and Competitiveness (MINECO) with a Juan de la Cierva contract (JCI-2010-06397) and a FPU grant (AP-2009-3711). S.B received additional funds from the Spanish Research Council (CSIC) (JAEDOC027) and the MICECO-funded project MED_FORESTREAM (CGL2011-30590). M. Ribot was funded by a technical training contract from the MINECO-funded project ISONEF (CGL2008-05504-C02-02/BOS) and MED_FORESTREAM. Additional financial support was provided by the European Union-funded project REFRESH (FP7-ENV-2009-1-244121) and the MINECO-funded project MONTES-Consolider (CSD 2008-00040). The Vichy Catalan Company, the Regàs family and the Catalan Water Agency (ACA) graciously gave us permission for at the Font del Regàs catchment.

References

Alexander, R. B., Böhlke, J. K., Boyer, E. W., David, M. B., Harvey, J. W., Mulholland, P. J., Seitzinger, S. P., Tobias, C. R., Tonitto, C., and Wollheim, W. M.. Dynamic modeling of nitrogen losses in river networks unravels the coupled effects of hydrological and biogeochemical processes. Biogeochemistry, 93, 91-116, 2009.

Asano, Y., Uchida, T.M., Mimasu, Y., and Ohte, N. Spatial patterns of stream solute concentrations in a steep mountainous catchment with a homogeneous landscape. Water Resour. Res., 45, W10432, doi: 10.1029/2008WR007466, 2009.

650 Àvila, A., and Rodà, F. Changes in atmospheric deposition and streamwater chemistry
651 over 25 years in undisturbed catchments in a Mediterranean mountain environment.
652 Sci. Total Environ., 434, 18-27, 2012.
653 Baethgen, W., and Alley, M. A manual volorimetric procedure for ammonium nitrogen
654 in soil and plant Kjeldahl Digests. Commun. Soil Sci. Plan., 20, 961–969, 1989.
655 Bernal, S., and Sabater, F. Changes in stream discharge and solute dynamics between
656 hillslope and valley-bottom intermittent streams. Hydrol. Earth Syst. Sci., 16, 1595-
657 1605, 2012.
658 Bernal, S., von Schiller, D., Martí, E., Sabater, F. In-stream net uptake regulates
659 inorganic nitrogen export from catchment under base flow conditions. J. Geophys.
660 Res., 117, G00N05, doi:10.1029/2012JG001985, 2012.
661 Bernhardt, E.S., Hall, R.O., and Likens, G.E. Whole-system estimates of nitrification
662 and nitrate uptake in streams of the Hubbard Brook experimental forest. Ecosystems,
663 5, 419-430, 2002.
664 Bernhardt, E.S., Likens, G.E., Buso, D.C., and Driscoll, C.T. In-stream uptake dampens
665 effects of major forest disturbance on watershed nitrogen export. P. Natl. Acad. Sci.
666 USA, 100, 10304-10308, 2003.
667 Bohlen, P.J., Groffman, P.M., Driscoll, C.T., Fahey, T.J., and Siccama, T.G. Plant-soil-
668 microbial interactions in a northern hardwood forest. Ecology, 82, 965-978, 2001.
669 Bormann, F.H. and Likens, G.E. Nutrient cycling. Science,155, 424-429, 1967.
670 Brookshire, E.N.J., Valett, H.M., and Gerber, S.G. Maintenance of terrestrial nutrient
671 loss signatures during in-stream transport. Ecology, 90, 293-299, 2009.
672 Butturini, A., Bernal, S., Nin, E., Hellín, C, Rivero, L., Sabater, S., and Sabater, F.
673 Influences of stream groundwater hydrology on nitrate concentration in unsaturated

674 riparian area bounded by an intermittent Mediterranean stream. Water Resour. Res.,
675 39, 1110, doi:10.1029/2001WR001260, 2003.
676 Castro-Díez, P., Valle, G., González-Muñoz, N., Alonso, A. 2014. Can the life-history
677 strategy explain the success of the exotic trees *Ailanthus altissima* and *Robinia*
678 *pseudoacacia* in Iberian floodplain forests? PLOS One 9, doi:
679 10.1371/journal.pone.0100254.
680 Compton, J.E., Robbin Church, M., Larned S.T., and Hogsett, W.E. Nitrogen export
681 from forested watershed in the Oregon Coast Range: the role of N_2-fixing red alder.
682 Ecosystems, 6, 773-785, 2003.
683 Covino, T.P., and McGlynn, B.L. Stream gains and losses across a mountain-to-valley
684 transition: impacts on watershed hydrology and stream water chemistry. Water
685 Resour. Res., 43, W10431, doi:10.1029/2006WR005544, 2007.
686 Covino, T.P., McGlynn, B.L., and Baker, M. Separating physical and biological nutrient
687 retention and quantifying uptake kinetics from ambient to saturation in successive
688 mountain stream reaches. J. Geophys. Res., 115, G04010,
689 doi:10.1029/2009/JG001263, 2010.
690 Dent, C.L., and Grimm, N.B. Spatial heterogeneity of stream water nutrient
691 concentrations over successional time. Ecology, 80, 2283-2298, 1999.
692 Dent, C.L., Grimm, N.B. Martí, E., Edmonds, J.W., Henry, J.C., and Welter, J.R.
693 Variability in surface-subsurface hydrologic interactions and implications for
694 nutrient retention in an arid-land stream. J. Geophys. Res., 112, G04004,
695 doi:10.1029/2007JG000467, 2007.
696 Ensign, S.H., and Doyle, M.W. Nutrient spiraling in streams and river networks. J.
697 Geophys. Res., 111, G04009, doi:10.1029/2005JG00114, 2006.

698 Finlay, J. C., Hood, J. M., Limm, M. P., Power, M. E., Schade, J. D., and Welter, J. R..
699 Light-mediated thresholds in stream-water nutrient composition in a river network.
700 Ecology, 92, 140-150, 2011.
701 Gordon N.D., McMahon T.A., Finlayson B.L., Gippel, C.J., and Nathan, R.J. Stream
702 hydrology: an introduction for ecologists. Wiley, West Sussex, UK, 2004.
703 Groffman, P.M., Gold, A.J., and Simmons, R.C. Nitrate dynamics in riparian forests:
704 microbial studies. J. Environ. Qual., 21, 666-671, 1992.
705 Harms, T.K., and Grimm, N.B. Hot spots and hot moments of carbon and nitrogen
706 dynamics in a semiarid riparian zone. J. Geophys. Res., 113, G01020,
707 doi:10.1029/2007JG000588, 2008.
708 Hedin, L.O., von Fisher, J.C., Ostrom, N.E., Kennedy, B.P., Brown, M.G., and
709 Robertson, G.P. Thermodynamic constraints on nitrogen transformations and other
710 biogeochemical processes at soil-stream interfaces. Ecology, 79, 684-703, 1998.
711 Helfield, J.M., and Naiman, R.J. Salmon and alder as nitrogen sources to riparian
712 forests in a boreal Alaskan watershed. Oecologia, 133, 573-582, doi:
713 10.1007/s00442-002-1070-x, 2002.
714 Hill, A.R., Labadia, C.F., and Sanmugadas, K. Hyporheic zone hydrology and nitrogen
715 dynamics in relation to the streambed topography of a N-rich stream.
716 Biogeochemistry, 42, 285-310, 1998.
717 Hill, W.R., Mulholland, P.J., and Marzolf, E.R. Stream ecosystem response to forest
718 leaf emergence in spring. Ecology, 82, 2306-2319, 2001.
719 Houlton, B.Z., Driscoll, C.T., Fahey, T.J., Likens, G.E., Groffman, P.M., Bernhardt,
720 E.S., and Buso, D.C. Nitrogen dynamics in ice-storm-damaged forest ecosystems:
721 implications for nitrogen limitation theory. Ecosystems, 6, 431-443, 2003.

722 Institut Cartografic de Catalunya (ICC). Orthophotomap of Catalunya 1:25 000.
723 Generalitat de Catalunya. Departament de Política Territorial i Obres, 2010.
724 Jencso, K.G., McGlynn, B.L., Gooseff, M.N., Bencala, K.E., and Wondzell, S.M.
725 Hillslope hydrologic connectivity controls riparian groundwater turnover:
726 implications of catchment structure for riparian buffering and stream water sources.
727 Water Resour. Res., 46, W10524, doi:10.1029/2009WR008818, 2010.
728 Johnson, C.E., Driscoll, C.T., Siccama, T.G., and Likens, G.E. Element fluxes and
729 landscape position in a northern hardwood forest watershed ecosystem. Ecosystems,
730 3, 159-184, 2000.
731 Jones, J.B. Jr., Fisher, S.G., and Grimm, N.B. Nitrification in the hyporheic zone of a
732 desert stream ecosystem. J. North Am. Benthological Soc., 14, 249-258, 1995.
733 Keeney D.R., and Nelson D.W. Nitrogen-inorganic forms. Methods of soil analysis.
734 Part 2. In: Agronomy Monography 9. ASA and SSSA. Madison, WI. pp. 643–698,
735 1982.
736 Lawrence, G.B., Lovett, G.M., and Baevsky, Y.H. Atmospheric deposition and
737 watershed nitrogen export along an elevational gradient in the Castkills Mountains,
738 New York. Biogeochemistry, 50, 21-43, 2000.
739 Lewis, D. B., Schade, J. D., Huth, A. K., and Grimm, N. B. The spatial structure of
740 variability in a semi-arid, fluvial ecosystem. Ecosystems, 9, 386-397, 2006.
741 Likens, G.E. and Buso, D.C. Variation in streamwater chemistry throughout the
742 Hubbard Brook Valley. Biogeochemistry, 78, 1-30, doi: 10.1007/s10533-005-2024-
743 2, 2006.
744 Lowrance, R., Altier, L. S., Newbold, J. D., Schnabel, R. R., Groffman, P. M., Denver,
745 J. M., Correl. D. L., Gilliam, J. W., Robinson, J. L., Brinsfield, R. B., Staver, K. W.,

746 Locas, W., and Todd, A. H. Water quality functions of riparian forest buffers in
747 Chesapeake Bay watersheds. Environ. Manag., 21, 687-712, 1997.
748 Lupon, A., Martí, E., Sabater, F. and Bernal, S. Green light: gross primary production
749 influences seasonal stream N export by controlling fine-scale N dynamics. Ecology
750 (in review), 2014.
751 Martí, E., Fisher, S.G., Schade, J.D., and Grimm, N.B. Flood-frequency and stream-
752 riparian linkages in arid lands, in: Streams and ground waters. Jones, J.B. and
753 Mulholland, P.J. (Eds), Academic Press, London, UK, 2000.
754 Mayer, P.M., Reynolds, S.K., Marshall, Jr., McCutchen, D., and Canfield, T.J. Meta-
755 Analysis of nitrogen removal in riparian buffers. J. Environ. Qual. 36, 1172-1180,
756 doi:10.2134/jeq2006.0462, 2007.
757 McClain, M.E., Boyer, E.W., Dent, C.L., Gergel, S.E., Grimm, N.B., Groffman, P.M.,
758 Hart, S.C., Harvey, J.W., Johnston, C.A., Mayorga, E., McDowell, W.H., and Pinay,
759 G. Biogeochemical hot spots and hot moments at the interface of terrestrial and
760 aquatic ecosystems. Ecosystems, 6, 301–312, 2003.
761 Meyer, J. L., and Likens, G. E. Transport and transformation of phosphorus in a forest
762 stream ecosystem. Ecology 60, 1255-1269, 1979.
763 Mineau, M. M., Baxter, C. V., and Marcarelli, A. M. A non-native riparian tree
764 (*Elaeagnus angustifolia*) changes nutrient dynamics in streams. Ecosystems, 14, 353-
765 365, 2011.
766 Morrice, J.A., Valett, H.M., Dahm, C.N., and Campana, M.E.: Alluvial characteristics,
767 groundwater-surface water exchange and hydrological retention in headwaters
768 streams, Hydrol. Process., 11, 253-267, 1997.
769 Murphy, J. and J.P. Riley. A modified single solution method for determination of
770 phosphate in natural waters. Anal. Chim. Acta, 27, 31-36, 1962.

771 Nadal-Sala, D, Sabaté, S., Sánchez-Costa, E., Boumghar, A., and Gracia, C.A.,
772 Different responses to water availability and evaporative demand of four co-
773 occurring riparian tree species in N Iberian Peninsula. Temporal and spatial sap flow
774 patterns. Acta Hortic. 991, 215-222, 2013.
775 Payn, R. A., Gooseff, M. N., McGlynn, B. L., Bencala, K. E., and Wondzell, S. M.
776 Channel water balance and exchange with subsurface flow along a mountain
777 headwater stream in Montana, United States. Water Resour. Res., 45, W11427,
778 doi:10.1029/2008WR007644, 2009.
779 Peterson, B. J., Wollheim, W. M., Mulholland, P. J., Webster J. R., Meyer, J. L., Tank,
780 J. L., Martí, E., Bowden, W. B., Valett, H. M., Hershey, A. E., McDowell, W. H.,
781 Dodds, W. K., Hamilton, S. K., Gregory, S., and Morrall, D. D. Control of nitrogen
782 export from watersheds by headwater streams. Science, 292, 86–90, 2001.
783 Roberts, B.J., and Mulholland, P.J. In-stream biotic control on nutrient biogeochemistry
784 in a forested stream, West Fork of Walker Branch. J. Geophys. Res., 112, G04002,
785 doi:10.1029/2007JG000422, 2007.
786 Ross, D.S., Shanley, J.B., Campbell, J.L., Lawrence, G.B., Bailey, S.W., Likens, G.E.,
787 Wemple, B.C., Fredriksen, G., and Jamison, A.E. Spatial patterns of soil nitrification
788 and nitrate export from forested headwaters in the northeastern United States. J.
789 Geophys. Res., 117, G01009, doi: 10.1029/2011JG001740, 2012.
790 Sabater, S., Butturini, A., Clement, J.C., Burt, T., Dowrick, D., Hefting, M., Maître, V.,
791 Pinay, G., Postolache, C., Rzepecki, M., and Sabater, F. Nitrogen removal by
792 riparian buffers along a European climatic gradient: patterns and factors of variation.
793 Ecosystems, 6, 20-30, 2003.

794 Scanlon, T.M., Ingram, S.P., and Riscassi, A.L. Terrestrial and in-stream influences on
795 the spatial variability of nitrate in a forested headwater catchment. J. Geophys. Res.,
796 115, G02022, doi:10.1029/2009JG001091, 2010.
797 Starry, O. S., Valett, H. M., and Schreiber, M. E. Nitrification rates in a headwater
798 stream: influences of seasonal variation in C and N supply. J. North Am.
799 Benthological Soc., 24, 753-768, 2005.
800 Stock, W.D., Wienand, K.T., and Baer, A.C. Impacts of invading N_2-fixing acacia
801 species on patterns of nutrient cycling in two Cape ecosystems: evidence from soil
802 incubation studies and ^{15}N natural abundance values. Oecologia, 101, 375-382, 1995.
803 Strauss, E.A., and Lamberti, G.A. Regulation of nitrification in aquatic sediments by
804 organic carbon. Limnol. Oceanogr., 45, 1854-1859, 2000.
805 Technicon. Technicon Instrument System, in : Technicon Method Guide, Technicon,
806 ed.Tarrytown, New York, 1976.
807 Uehlinger, U. Resistance and resilience of ecosystem metabolism in a flood-prone river
808 system. Freshwater Biol., 45, 319-332, 2000.
809 Valett, H.M., Morrice, J.A., Dahm, C.N. and Campana, M.E. Parent lithology, surface-
810 groundwater exchange and nitrate retention in headwater streams. Limnol.
811 Oceanogr., 41, 333-345, 1996.
812 Vidon, P., and Hill, A.R. Landscape controls in nitrate removal in stream riparian zones.
813 Water Resour. Res., 40, W03201, doi:10.1029/2003WR002473, 2004.
814 Vidon, P.G.F., Craig, Al., Burns, D., Duval, T.P., Gurwick, N., Inamdar, S., Lowrance,
815 R., Okay, J., Scott, D., and Sebestyen, S. Hot spots and hot moments in riparian
816 zones: potential for improved water quality management. J. Am. Water Resour.
817 Assoc., 46, 278-298, 2010.

von Schiller, D., Bernal, S., and Martí, E. A comparison of two empirical approaches to estimate in-stream net nutrient uptake. Biogeosciences, 8, 875-882, 2011.

von Schiller, D., Bernal, S., Sabater, S., and Martí, E. A round-trip ticket: the importance of release processes for in-stream nutrient spiraling. Freshwater Science, DOI: 10.1086/679015, 2015.

Wollheim, W. M., Vörösmarty, C. J., Peterson, B. J., Seitzinger, S. P., and Hopkinson, C. S. Relationship between river size and nutrient removal. Geophys. Res. Lett., 33, L06410, doi:10.1029/2006GL025845, 2006.

Zar, J. H. Biostatistical analysis. Prentice-Hall/Pearson, Ed. 5th Edition. Upper Saddle River, N.J., 2010.

Tables

Table 1. Median and interquartile range [25th, 75th percentiles] of stream and riparian groundwater solute concentrations for the dormant and vegetative period. The number of cases is shown in parenthesis for each group. For each variable, the asterisk indicates statistically significant differences between the two water bodies (Wilcoxon paired rank sum test, $p < 0.01$).

		Stream	Riparian groundwater
Dormant	Cl^- (mg L^{-1})	7.6 [6.5, 8] (60)	7.7 [7.2, 8.8] (57)*
	$N\text{-}NO_3^-$ (μg N L^{-1})	192 [159, 262] (60)	194 [109, 298] (56)
	$N\text{-}NH_4^+$ (μg N L^{-1})	8.9 [6.5, 10.3] (60)	19 [13.8, 34.2] (56)*
	SRP (μg P L^{-1})	7.6 [4.5, 11.7] (60)	8 [6, 20] (51)
	DO (mg L^{-1})	12.9 [11.5, 16] (60)	3.5 [1.5, 4.6] (54)*
Vegetative	Cl^- (mg L^{-1})	8.8 [7.9, 13.5] (100)	10.1 [8.6, 15] (98)*
	$N\text{-}NO_3^-$ (μg N L^{-1})	223 [155, 282] (102)	168 [77, 264] (98)*
	$N\text{-}NH_4^+$ (μg N L^{-1})	10 [8.7, 12.8] (103)	27 [18.2, 37.1] (101)*
	SRP (μg P L^{-1})	16.5 [11.7, 21.3] (103)	14.1 [9.3, 23.3] (97)
	DO (mg L^{-1})	9.9 [9.1, 11.1] (84)	1.7 [0.8, 2.5] (98)*

836 **Table 2**. Spearman ρ coefficient between stream water and riparian groundwater solute
837 concentrations for each period and for the whole data set collected at the Font del Regàs
838 during the study period. The relative root mean square error (RRMSE) indicates
839 divergences from the 1:1 line. The number of cases is shown in parenthesis for each
840 variable. ns, no significant.

	Dormant			Vegetative			All data		
	ρ	RRMSE (%)	n	ρ	RRMSE (%)	n	ρ	RRMSE (%)	n
Cl^-	0.78*	2.1	53	0.8*	2.9	98	0.84*	2.8	151
$N\text{-}NO_3^-$	0.48*	8.1	57	0.34*	8.3	101	0.37*	6	158
$N\text{-}NH_4^+$	ns	11.7	57	ns	9.1	101	ns	7.3	158
SRP	ns	17.9	57	0.43*	5.5	101	0.41*	7.3	158

841 *p<0.001

842

843

844 **Table 3**. Median and interquartile range [25th, 75th percentile] of in-stream net nutrient
845 uptake flux (F_{sw}) and the potential of F_{sw} to modify solute input fluxes ($|F_{sw} \cdot x / F_{in}|$) for
846 the two spatial scales considered (stream segment and whole reach) during the study
847 period. n = 150 and 10 for segments and whole-reach data sets, respectively.

		By segment	By whole reach
F_{sw} ($\mu g\ m^{-1}\ s^{-1}$)	Cl^-	6 [-37, 80]	12 [2, 33]
	$N\text{-}NO_3^-$	-0.43 [-4.4, 1.3]	-0.97 [-3.4, 1.6]
	$N\text{-}NH_4^+$	0.17 [-0.06, 0.63]	0.2 [-0.02, 1.1]
	SRP	0 [-0.6, 0.21]	-0.06 [-0.21, 0.01]
$\lvert F_{sw} \cdot x / F_{in} \rvert$ (%)	Cl^-	3 [1, 10]	4 [2, 9]
	$N\text{-}NO_3^-$	6 [2, 14]	24 [8, 67]
	$N\text{-}NH_4^+$	18 [9.5, 35]	48 [25, 71]
	SRP	20.5 [3.4, 41]	15.5 [6, 66]

848
849

850 **Table 4**. Median and interquartile range [25th, 75th percentile] of the relative
851 contribution of inputs from upstream (F_{top}/F_{in}), net riparian groundwater ($F_{gw}>0/F_{in}$),
852 tributaries (F_{ef}/F_{in}), and in-stream release ($F_{sw}<0/F_{in}|$) to stream solute fluxes. For each
853 solute, different letters indicate statistically significant differences between solute
854 sources (Mann Whitney test with post-hoc Tukey test, $p > 0.01$). n = 10 for the 4
855 solutes.

Relative contribution (%)	Cl^-	$N\text{-}NO_3^-$	$N\text{-}NH_4^+$	SRP
Upstream	15 [12, 17]^{B}	22 [20, 35]^{A}	8 [6, 13]^{BC}	11 [6, 17]^{B}
Riparian Groundwater	28 [14, 38]^{B}	17 [5, 47]^{A}	63 [43, 75]^{A}	21 [7, 38]^{AB}
Tributaries	59 [46, 69]^{A}	22 [19, 24]^{A}	21 [17, 30]^{B}	34 [26, 50]^{A}
In-stream Release	0 [0, 0.3]^{C}	22 [0, 50]^{A}	0 [0, 6]^{C}	19 [0, 55]^{B}

856
857

858

859 **Figures**

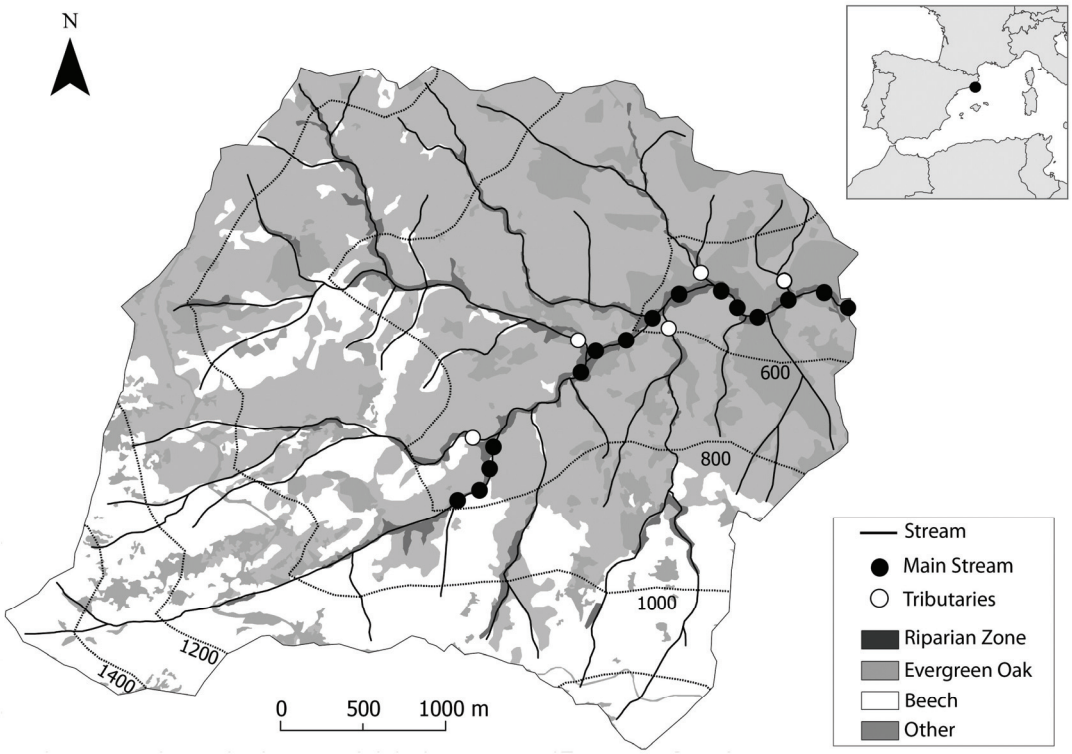

860

861

862 **Figure 1**. Map of the Font del Regàs catchment within the Montseny Natural Park (NE,
863 Spain). The vegetation cover and the main stream sampling stations along the 3.7-km
864 reach are indicated. There were 5 and 10 sampling stations along the 2nd and 3rd order
865 sections, respectively. Four permanent tributaries discharged to the main stream from
866 the upstream- to the downstream-most site (white circles). Additional water samples
867 were collected from a small tributary draining through the inhabited area at the lowest
868 part of the reach. The remaining tributaries were dry during the study period.

869

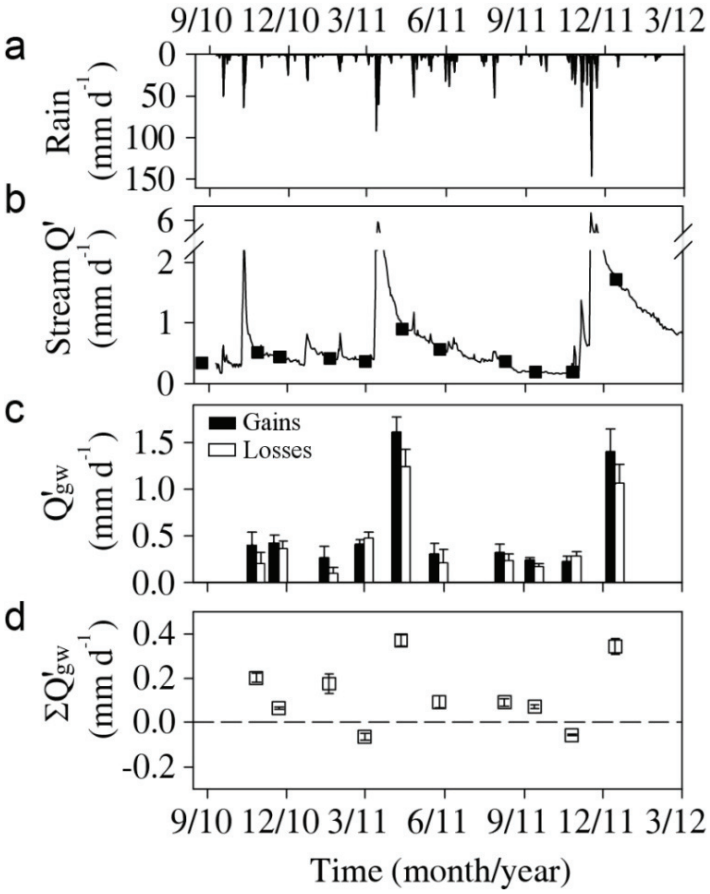

870

871 **Figure 2**. Temporal pattern of area-specific (a) rainfall, (b) stream discharge, (c) whole-
872 reach gross hydrological gains and losses, and (d) cumulative net groundwater inputs at
873 the downstream-most site. Black squares in (b) are dates of field campaigns. Error bars
874 in (c) and (d) show the uncertainty associated with the empirical estimation of *Q* from
875 tracer slug additions. Error bars in (b) are smaller than the symbol size.

876

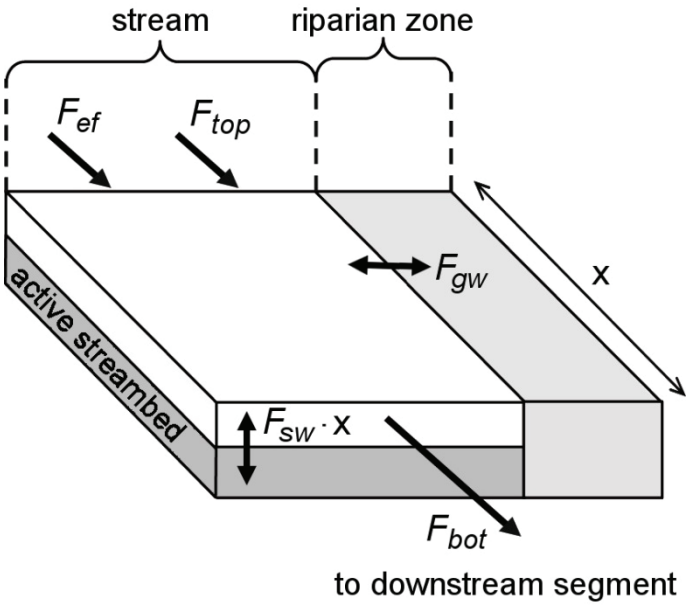

Figure 3. Conceptual representation of nutrient fluxes considered to estimate in-stream net nutrient uptake for each stream segment ($F_{sw} \cdot x$, Equation 2). For each segment of length x, the considered nutrient input fluxes were upstream (F_{top}) and tributaries (F_{ef}). Nutrient fluxes exiting the stream segment (F_{bot}) were F_{top} for the contiguous downstream segment. Riparian groundwater nutrient fluxes could either enter ($F_{gw} > 0$) or exit ($F_{gw} > 0$) the stream. Nutrient fluxes for each component were estimated by multiplying its water flux (Q) by its nutrient concentration (C). In-stream net nutrient uptake ($F_{sw} \cdot x$) is the result of gross nutrient uptake and release by the active streambed. $F_{sw} \cdot x$ can be positive (gross uptake > release), negative (gross uptake < release), or nil (gross uptake ~ release). See text for details.

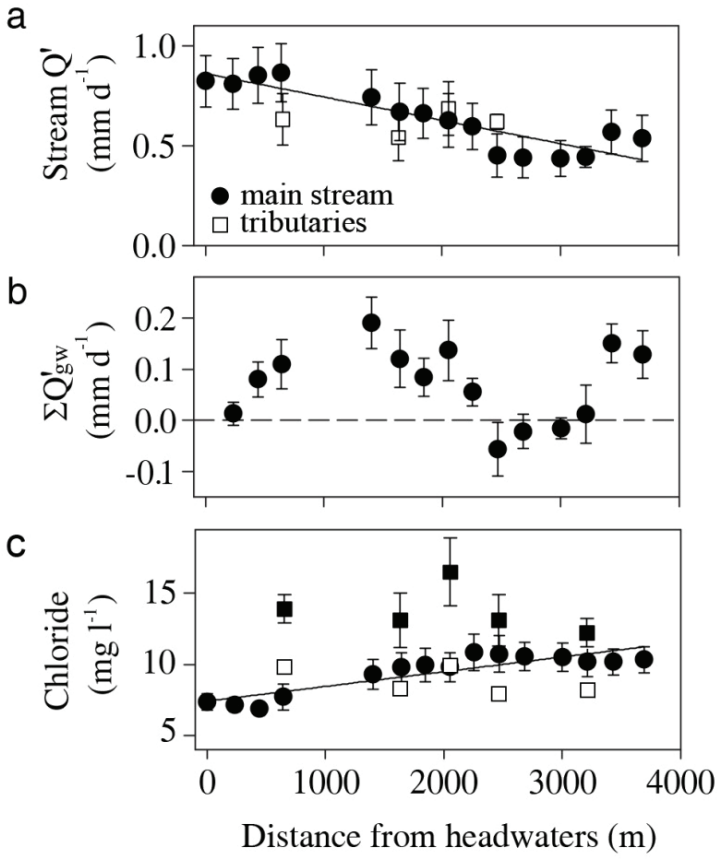

Figure 4. Longitudinal pattern of (a) area-specific stream discharge, (b) cumulative area-specific net groundwater inputs along the reach, and (c) stream chloride concentration. Symbols are average and standard error (whiskers) for the study period. Squares are values for tributaries. Stream chloride concentration in tributaries is shown separately for the dormant (white) and vegetative (black) period. Tributaries showed no differences in discharge between the two periods. Model regressions are indicated with a solid line only when significant (tributaries not included in the model).

900

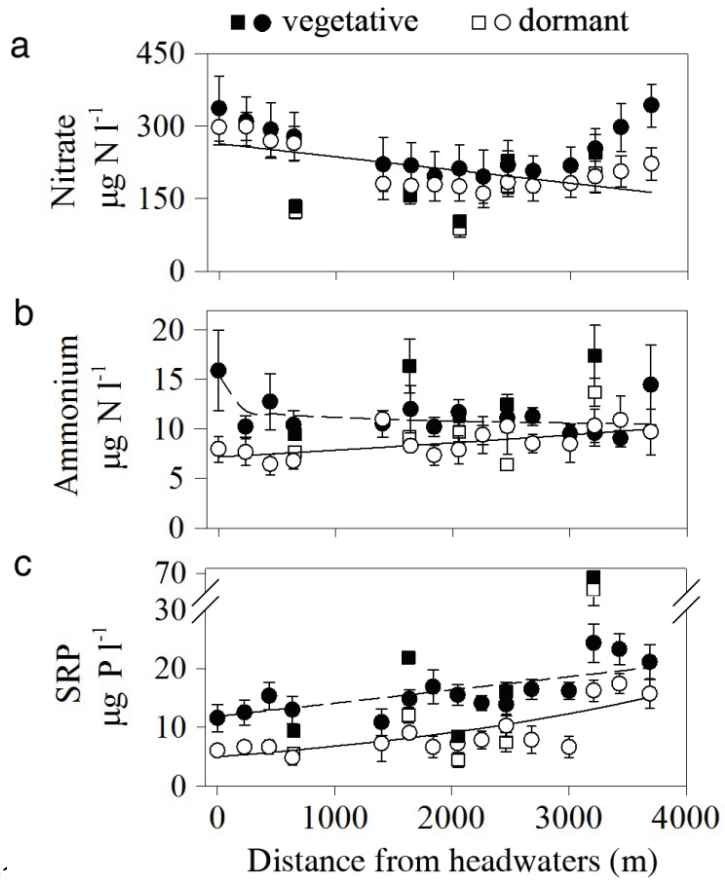

90:

902

903 **Figure 5.** Longitudinal pattern of stream nutrient concentrations for (a) nitrate, (b)

904 ammonium, and (c) solute reactive phosphorus at Font del Regàs. Symbols are average

905 and standard error (whiskers) for the main stream (circles) and tributaries (squares).

906 Lines indicate significant longitudinal trends for the dormant (solid) and vegetative

907 (dashed) period (tributaries not included in the model).

908

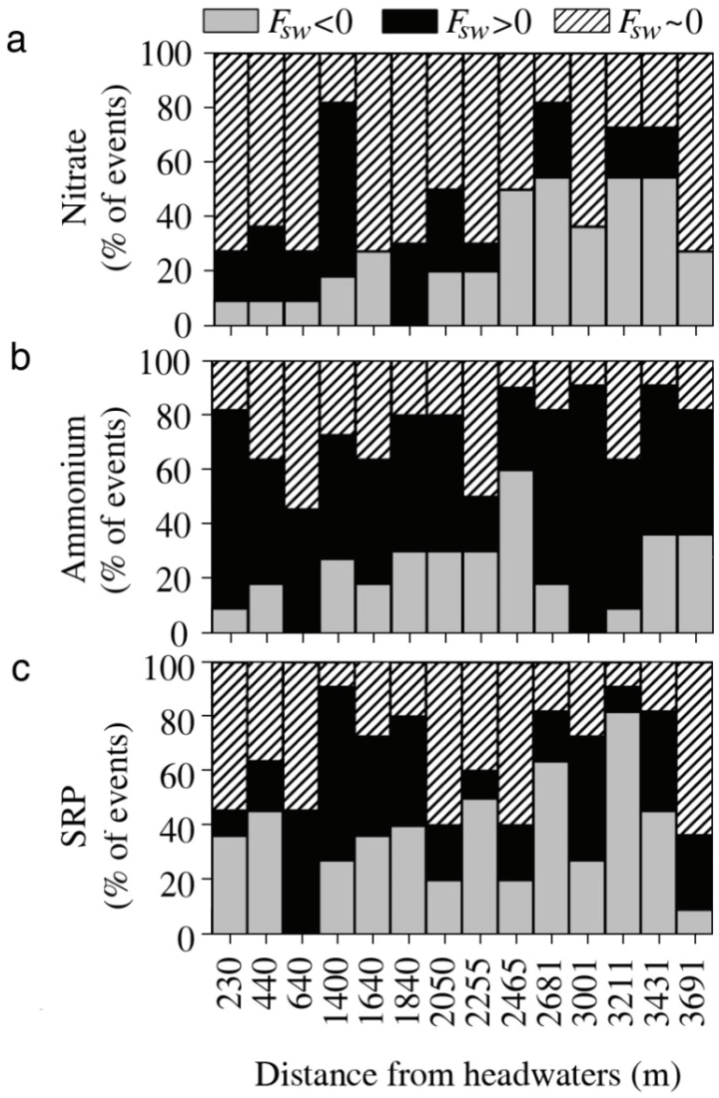

Figure 6. Frequency of dates for which $F_{sw} < 0$ (gross uptake < release), $F_{sw} > 0$ (gross uptake > release), and $F_{sw} \sim 0$ (gross uptake ~ release) for (a) nitrate, (b) ammonium, and (c) soluble reactive phosphorus for the 14 contiguous segments along the study reach from August 2010 to December 2011 (n = 11). The frequency is expressed as number of events in relative terms.

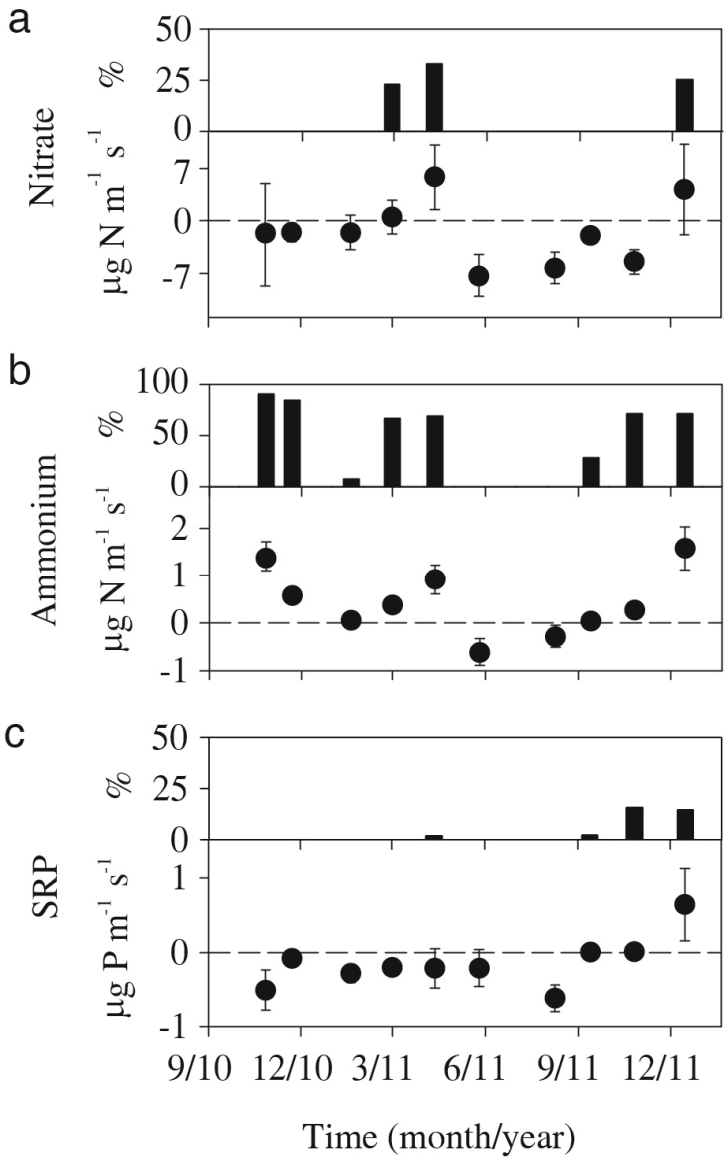

Figure 7. Temporal pattern of in-stream net nutrient uptake (F_{sw}, in μg m^{-1} s^{-1}) for (a) nitrate, (b) ammonium, and (c) soluble reactive phosphorus at the whole-reach scale. Whiskers are the uncertainty associated with the estimation of stream discharge from slug tracer additions. $F_{sw} > 0$ indicates that gross uptake prevailed over release, while $F_{sw} < 0$ indicates the opposite. For those cases for which $F_{sw} > 0$, the contribution of in-stream net nutrient uptake to reduce stream nutrient fluxes ($F_{sw} \cdot x/F_{in}$, in %) is shown (black bars).

Supplementary Figures

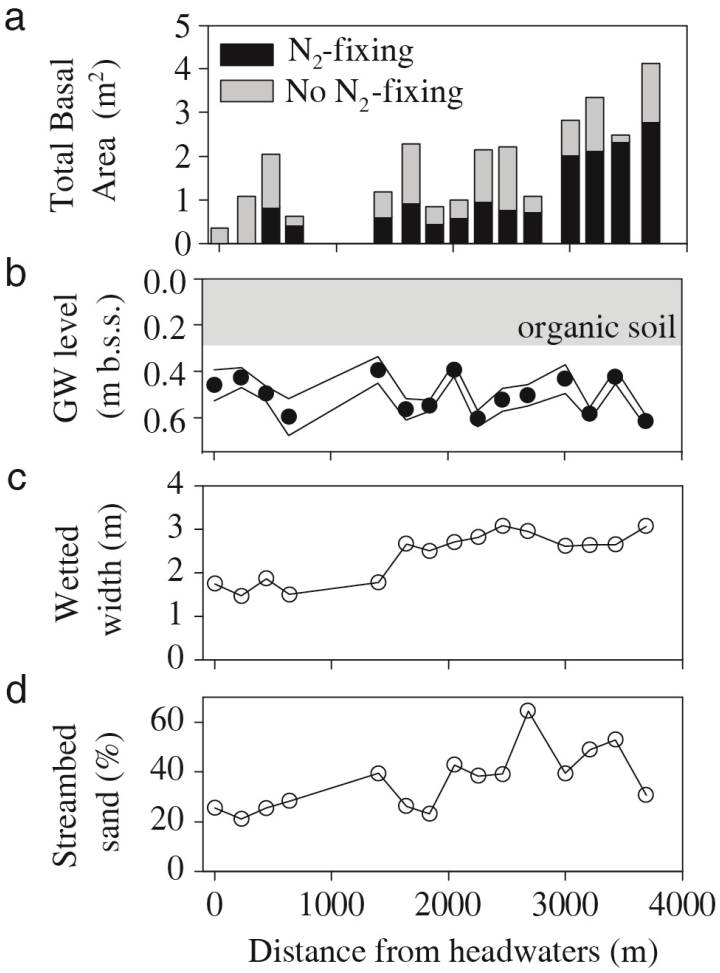

Figure S1. (a) Total basal area of riparian trees, (b) mean riparian groundwater level (in m below the soil surface), (c) stream wetted width, and (d) percentage of sands in streambed for each sampling site along the study reach. Different colors in (a) indicate the basal area of N_2- and no N_2-fixing trees. The solid lines in (b) are the 95% lower and upper values of the riparian groundwater level.

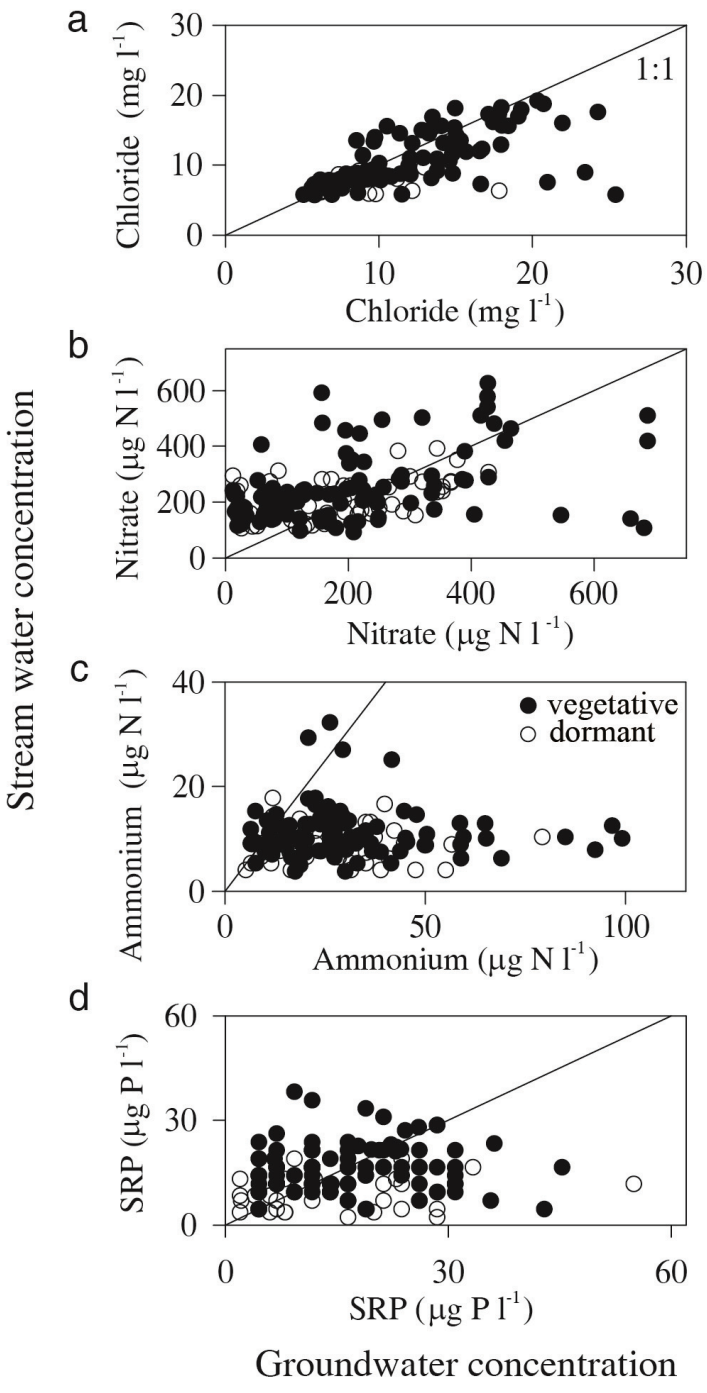

936

937 **Figure S2.** Relationship between riparian groundwater and stream water concentrations
938 for (a) chloride, (b) nitrate, (c) ammonium, and (d) soluble reactive phosphorus at each
939 sampling site and for each sampling date at Font del Regàs. The 1:1 line is indicated in
940 black.